Anal. Chem. **2009,** *81,* 2633–2643

Selective Histamine Piezoelectric Chemosensor Using a Recognition Film of the Molecularly Imprinted Polymer of Bis(bithiophene) Derivatives

Agnieszka Pietrzyk,[†] Subramanian Suriyanarayanan,[†] Wlodzimierz Kutner,*[,†,‡] Raghu Chitta,[§] and Francis D'Souza*[,§]

Institute of Physical Chemistry, Polish Academy of Sciences, Kasprzaka 44/52, 01-224 Warsaw, Poland, Faculty of Mathematics and Natural Science, School of Science, Cardinal Stefan Wyszynski University, Dewajtis 5, 01-815 Warsaw, Poland, and Wichita State University, 1845 Fairmount, Wichita, Kansas 67260-0051

A histamine piezoelectric (acoustic) sensor using a molecularly imprinted polymer (MIP) film has been devised and tested. The sensor comprises an electrodeposited MIP film as the recognition element and a 10 MHz AT-cut shear-thickness-mode bulk-acoustic-wave quartz crystal resonator with Pt film electrodes as the signal transducer. Preparation of the sensing film involved two consecutive electrochemical polymerizations, performed under cyclic voltammetric conditions, with the use of a supporting electrolyte of 0.1 M tetra-*n*-butylammonium perchlorate in acetonitrile. First, a poly(bithiophene) barrier film was deposited by electropolymerization on the Pt/quartz resonator to prevent histamine electro-oxidation and avoid possible contamination of the Pt electrode surface. Next, the histamine-templated MIP film was deposited by electropolymerization on top of this barrier film. For that purpose, two functional monomers of bis(bithiophene) derivatives, i.e., one bearing the 18-crown-6 and the other dioxoborinane substituent, were copolymerized in the presence of the histamine template. The consecutive growth of both these overlaid films was monitored with an electrochemical quartz crystal microbalance (EQCM). Subsequently, the histamine was extracted from MIP with 0.01 M NaOH for 12 h. The UV−vis and X-ray photoelectron spectroscopic measurements confirmed the completeness of the removal of the histamine template from the MIP film. The analytical performance of the chemosensor was assessed under flow injection analysis (FIA) conditions using the carrier 0.5 M HEPES buffer (pH = 7.5) solution and the piezoelectric microgravimetry detection at QCM. The negative peaks of resonant frequency linearly decreased with the increase of the histamine concentration in the range 10−100 mM for 150 μL/min flow rate, and 100 μL volume of the injected sample. The sensitivity of the chemosensor (0.33 Hz/mM) was more than twice as that of the chemosensor without the poly(bithiophene) barrier film (0.15 Hz/mM). The chemosensor performance was superior for selective histamine recognition if the poly(bithiophene) barrier film thickness exceeded 200 nm. The chemosensor discriminated histamine from functionally or structurally similar compounds, such as dopamine, tryptamine, and imidazole. Stability constants of the affinity complexes of MIP and analyte or the interfering agent were determined from kinetic studies. For the MIP−histamine complex, the stability constant thus evaluated was equal to 57.0 M^{-1} being much higher than those for the MIP−tryptamine and MIP−dopamine complexes determined to be 10.7, and 6.4 M^{-1}, respectively. The concentration limit of detection was as low as 5 nM histamine if the carrier solution flow rate was as low as 35 μL/min and the injection sample volume as large as 1 mL.

Histamine (Scheme 1) is one of the most important biogenic amines in clinical and food chemistry.[1] It acts as a neurohormone triggering a variety of allergic reactions.[2] In humans, abnormal histamine concentration manifests itself via dysfunctional symptoms, such as gastric disorder, mastocytosis, and chronic myelogenous leukemia.[3] Improperly handled fish or fish products may accumulate histamine above toxic levels in tissues and blood.[1]

In the histamine assay, selectivity is the major criterion for successful determination and, therefore, for sensing applications. Until now, histamine has been determined by batch immunoassays[2] or HPLC with the fluorescence,[4] UV−vis,[5] or electrochemical detection.[6] The HPLC determination, involving tedious separation, is time-consuming and relatively expensive. A determination

* To whom correspondence should be addressed. E-mail: wkutner@ichf.edu.pl (W.K.); Francis.DSouza@wichita.edu (F.D.S.).

[†] Polish Academy of Sciences.

[‡] Cardinal Stefan Wyszynski University.

[§] Wichita State University.

(1) Lehane, L.; Olley, J. *Int. J. Food Microbiol.* **2000**, *58*, 1–37.

(2) Holgate, S. T.; Robinson, C. ; Church, M. K. *Allergy: Principles and Practice*; C. V. Mosby Co.: St. Louis, MO, 1988.

(3) (a) Beaven, M. A. *Klin. Wochenschr.* **1982**, *60*, 873–881. (b) Beaven, M. A. In *Monographs in Allergy*; Karger, S., Ed.; Karger: Basel, Switzerland, 1978; Vol. 13.

(4) (a) Kuruma, K.; Sakano, T. *Anal. Sci.* **1999**, *15*, 489–492. (b) Lowe, D. R.; March, J. E.; James, J. E.; Karnes, H. T. *J. Liq. Chromatogr.* **1994**, *17*, 3563–3570. (c) Egger, D.; Reisbach, G.; Hultner, L. *J. Chromatogr., B* **1994**, *662*, 103–107.

(5) (a) Hockl, P. F.; Thyssen, S. M.; Libertun, C. *J. Liq. Chromatogr. Relat. Technol.* **2000**, *23*, 693–703.

(6) (a) Pihel, K.; Hsieh, S.; Jorgenson, J. W.; Wightman, R. M. *Anal. Chem.* **1995**, *67*, 4514–4521. (b) Washington, B.; Smith, M. O.; Robinson, T. J.; Olubadewo, J. O.; Ochillo, R. F. *J. Liq. Chromatogr.* **1991**, *14*, 2189–2200. (c) Okochi, M.; Yokouchi, H.; Nakamura, N.; Matsunaga, T. *Biotechnol. Bioeng.* **1999**, *65*, 480–484.

10.1021/ac8025652 CCC: $40.75
Published on Web 03/11/2009

Scheme 1. Acid–Base Equilibria of Histamine (1)

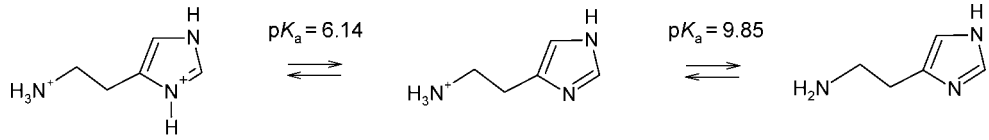

1b 1a 1

procedure involving GC/MS is most reliable; however, it requires histamine derivatization with organoflourine compounds.[7] Furthermore, histamine has been detected enzymatically using chronoamperometric biosensors based on histamine oxidase,[8] methylamine dehydrogenases,[9] or quinohemoprotein amine dehydrogenes.[10] These biosensors revealed serious disadvantages with respect to substrate specificity. Moreover, they suffered from interference of molecular oxygen.[8–11]

Molecular imprinting is a powerful technique for preparation of the polymeric recognition materials.[12] Molecularly imprinted polymers (MIPs) allow for the formation of binding sites, which are complementary in size and shape to those of the template or analyte molecule. These MIPs serve as recognition elements in respective chemosensors. One of the most appealing among the procedures of preparation of these films is electrochemical polymerization. This is because thickness, visco-elastic properties, porosity, and morphology of the resulting MIP film can conveniently be controlled by suitable selection of experimental conditions, such as the amount of charge transferred and solution pH as well as nature of solvent, supporting electrolyte, functional monomer, and cross-linking monomer. Moreover, electropolymerization does not require any further film treatment and, after template removal, the film can directly be applied for analyte determination.

A range of MIP-based chemosensors have already been devised.[13] These chemosensors utilized electrochemical, spectroscopic, acoustic (i.e., piezoelectric, PZ), and other analytical techniques for signal transduction. In this direction, the required chemosensor selectivity, sensitivity, and detectability can readily be gained by combining molecular imprinting of polymers and PZ transduction. A PZ resonator is very well suited for that purpose due to its very low limit of detection (LOD) reaching down to a subnanogram level.[14] As a result of this combination, efficiency of the MIP-PZ sensor can collectively be enhanced in terms of recognition, responsiveness, and binding.

Scheme 2. Structural Formulas of Functional Monomers for Preparation of Molecularly Imprinted Polymers by Electrochemical Polymerization[a]

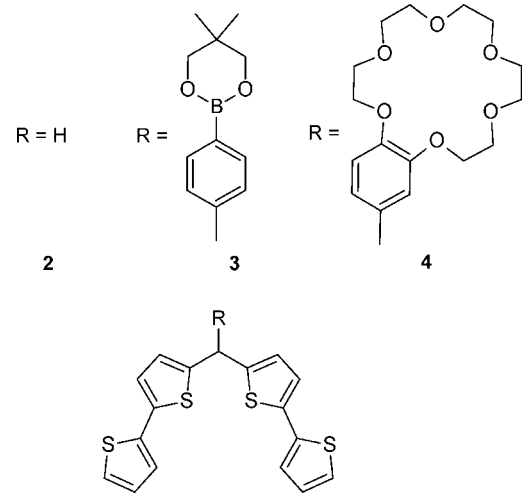

2 3 4

[a] Bis(2,2′-bithienyl)methane (**2**), bis(2,2′-bithienyl)-5,5-dimethyl-2-phenyl-[1,3,2]dioxaborinanemethane (**3**), bis(2,2′-bithienyl)-benzo-[18-crown-6]methane (**4**).

Herein, an acoustic histamine chemosensor has been devised and tested. This sensor uses a MIP film as a recognition element and a thickness-shear-mode bulk-acoustic-wave quartz resonator of a quartz crystal microbalance (QCM) as a signal transducer. Our aim was to construct a reproducibly operating chemosensor of appreciable stability, selectivity, sensitivity, and detectability. For that purpose, we have developed a new procedure of the MIP film preparation. Electrochemical polymerization, involving redox functional monomers that can prevailingly be polymerized under galvanostatic, potentiostatic, or voltammetric conditions, is one of the most elegant methods for preparation of the MIP films.[15] Bis(bithiophene) is a redox monomer, which can readily be polymerized under electrochemical conditions.[16] Moreover, it is relatively easy to derivatize with a range of the receptor type substituents at the methane carbon position to result in a whole library of useful functional monomers. The procedure adopted herein involves electrochemical copolymerization of functional monomers (Scheme 2) of the bis(bithiophene) methane derivatives bearing either dioxaborinane, **3**, or 18-crown-6, **4**, substituents, under cyclic voltammetry conditions, in the presence of the histamine template and redox functional monomers, desirably derivatives of bis(bithiophene).

Formation of selective binding sites in MIP is a crucial factor governing sensor selectivity. Histamine is built of the aliphatic

(7) (a) Payne, N.; Zirrolli, A.; Gerber, G. *Anal. Biochem.* **1988**, *178*, 414–420. (b) Navert, H.; Berube, R.; Wollin, A. *Can. J. Physiol. Pharmacol.* **1985**, *63*, 766–772. (c) Keyzer, J. J.; Wolthers, E. G.; Muskiet, F. A.; Breukelman, H.; Kauffman, H. F.; de Vries, K. *Anal. Biochem.* **1984**, *139*, 474–481. (d) Mita, H.; Yasueda, H.; Shida, T. *J. Chromatogr., B* **1980**, *181*, 153–159.

(8) (a) Niwa, O.; Kurita, R.; Hayashi, K.; Horiuchi, T.; Torimitsu, K.; Maeyama, K.; Tanizawa, K. *Sens. Actuators, B* **2000**, *67*, 43–51. (b) Iwaki, S.; Ogasawara, M.; Kurita, R.; Niwa, O.; Tanizawa, K.; Ohashi, Y.; Maeyama, K. *Anal. Biochem.* **2002**, *304*, 236–243.

(9) (a) Loughran, M. G.; Hall, J. M.; Turner, A. P. F.; Davidson, V. L. *Biosens. Bioelectron.* **1995**, *10*, 569–576. (b) Zeng, K.; Tachikawa, H.; Zhu, Z.; Davidson, V. L. *Anal. Chem.* **2000**, *72*, 2211–2215.

(10) Yamamoto, K.; Takagi, K.; Kano, K.; Ikeda, T. *Electroanalysis* **2001**, *13*, 375–379.

(11) Bao, L. L.; Sun, D. P.; Tachikawa, H.; Davidson, V. L. *Anal. Chem.* **2002**, *74*, 1144–1148.

(12) (a) Haupt, K. *Chem. Commun.* **2003**, 171–178. (b) Haupt, K.; Mosbach, K. *Chem. Rev.* **2000**, *100*, 2495–2504. (c) Wulff, G. *Angew. Chem., Int. Ed. Engl.* **1995**, *34*, 1812–1832.

(13) (a) Blanco-López, M. C.; Lobo-Castanón, M. J.; Miranda-Ordieres, A. J.; Tunón-Blanco, P. *Trends Anal. Chem.* **2004**, *23*, 36–48. (b) Piletsky, S. A.; Turner, A. P. F. *Electroanalysis* **2002**, *14*, 317–323. (c) Henry, O. Y. F.; Cullen, D. C.; Piletsky, S. A. *Anal. Bioanal. Chem.* **2005**, *382*, 947–956.

(14) Ávila, M.; Zougagh, M.; Ríos, Á.; Escarpa, A. *Trends Anal. Chem* **2008**, *27*, 54–65.

primary amine and a heteroaromatic imidazole ring moieties (Scheme 1). In the pH range between $pK_{a1} = 6.14$ and $pK_{a2} = 9.85$ of histamine, the aliphatic amine group is protonated yielding $-NH_3^+$. The 18-crown-6 moiety, **4**, of MIP served as a recognition site of this group (Scheme 3). Moreover, a lone electron pair of the nitrogen atom of the imidazole ring of histamine coordinated to the vacant orbital of the boron atom of the dioxaborinane group in this pH range. The electron-rich histamine molecule is responsible for the basic environment around the electron-deficient boron atom center inducing dioxaborinane−imidazole interactions and decreasing the working pH value of the sensor.[17]

For extraction of the histamine template from the MIP film, we used a strong base solution. In this solution, the proton is dissociated leaving the aliphatic amine group of histamine neutral. Therefore, the complex of the 18-crown-6 moiety and histamine dissociates.[17] Moreover, the coordination bond between the nitrogen atom of the imidazole moiety of histamine and the boron atom of the dioxaborinane moiety of the polymer is cleaved due to the formation of a new bond (B−OH) between the boron atom and hydroxy group from the employed basic solution.[17] In that way, the template-free MIP film became ready for determination of the histamine analyte. This determination was performed herein under flow injection analysis (FIA) conditions with the QCM detection using a buffer carrier solution of the pH value suitable for rebinding of histamine.

EXPERIMENTAL SECTION

Chemicals. Acetonitrile, 1,2-dichlorobenzene, histamine, and dopamine were purchased from Sigma-Aldrich (Milwaukee, WI). Tryptamine and imidazole were procured from Lancaster (Morecambe, U.K.). Trifluoroacetic acid (TFA), the HEPES buffer, and tetra-*n*-butylammonium perchlorate [(TBA)ClO_4] were purchased from Fluka (Buchs, Switzerland). NaOH and ethanol were obtained from Chempur (Piekary Slaskie, Poland). All chemicals were used as received.

Preparation of Bis(bithiophene) Functional Monomers. meso-*[4-(5,5-dimethyl-1,3,2-dioxaboran-2-yl)phenyl]bis(2,2′-bithienyl)methane. 2-(4-Formylphenyl)-5,5-dimethyl-1,3,2-dioxaborane (**3a**).* 2-(4-Formylphenyl)-5,5-dimethyl-1,3,2-dioxaborane (**3a**) was prepared according to the literature procedure with some modificatons.[18] That is, 4-formylphenylboronic acid (300 mg, 2 mmol) was added to 2,2-dimethylpropane-1,3-diol (237.56 mg, 2.281 mmol) in anhydrous THF (15 mL), and the mixture was stirred for 10 min at room temperature. The solvent was then evaporated under reduced pressure and the residue was dissolved in CH_2Cl_2, washed with H_2O, and dried over anhydrous Na_2SO_4. Evaporation of the solvent yielded pale yellow oil, which upon trituration with hexane followed by refrigeration, gave the desired product as a white solid. Yield: 428 mg (98%). ^{1}H NMR ($CHCl_3$-*d*): δ (in ppm) 10.05 (s, 1H, CHO), 7.95 (d, 2H, phenyl *H*), 7.85 (d, 2H, phenyl *H*), 3.79 (s, 4H, $2CH_2$), 1.02 (s, 6H, $2CH_3$).

Scheme 3. Excerpt of the Structural Formula of the Polymer Molecularly Imprinted with the Histamine Template

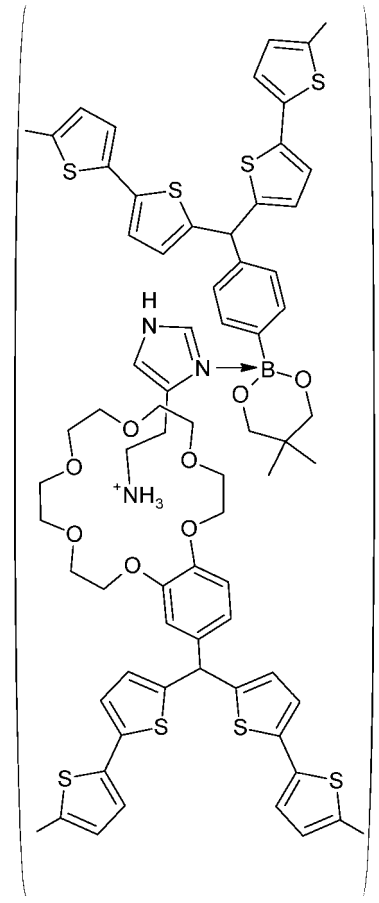

meso-*[4-(5,5-Dimethyl-1,3,2-dioxaboran-2-yl)phenyl]bis(2,2′-bithienyl)methane (**3**).* meso-[4-(5,5-Dimethyl-1,3,2-dioxaboran-2-yl)phenyl]bis(2,2′-bithienyl)methane (**3**) was prepared according to the described procedure[19] with some modifications. Namely, 2, 2′-bithiophene (1.54 g, 9.3 mmol) and **3a** (1.03 g, 4.72 mmol) were mixed with ethylene glycol (75 mL) and the mixture was stirred for 20 min under N_2. Next, 60% $HClO_4$ (10 mL, 0.091 mol) was added and the mixture was stirred for 16 h at 60 °C. Then, the reaction mixture was cooled and filtered, and the precipitate was washed with CH_2Cl_2. The resultant residue was washed with saturated Na_2CO_3 and water and then extracted with CH_2Cl_2. The organic phase was evaporated, and the obtained oily residue was purified by LC on a silica gel column using hexane: $CHCl_3$ (40:60, v/v) as the eluent. Yield: 743 mg (31%). ^{1}H NMR ($CHCl_3$-*d*): δ (in ppm) 7.78 (d, 2H, phenyl *H*), 7.35 (d, 2H, phenyl *H*), 7.16 (dd, 2H, bithiophene *H*), 7.08 (dd, 2H, bithiophene *H*), 7.01 (d, 2H, bithiophene *H*), 6.99−6.95 (m, 2H, bithiophene *H*), 6.74 (dd, 2H, bithiophene *H*), 5.76 (s, 1H, −CH−), 3.75 (s, 4H, $2CH_2$), 1.02 (s, 6H, $2CH_3$).^{13}C NMR ($CHCl_3$-*d*): δ (in ppm): 146.30, 145.41, 137.61, 137.04, 134.4,

(15) Malitesta, C.; Losito, I.; Zambonin, P. G. *Anal. Chem.* **1999**, *71*, 1366–1370.

(16) (a) Roncali, J. *Chem. Rev.* **1992**, *92*, 711–738. (b) Pei, Q.; Inganäs, O.; Gustafsson, G.; Granström, M.; Andersson, M.; Hjertberg, T.; Wennerström, O.; Österholm, J. E.; Laakso, J.; Järvinen, H. *Synth. Met.* **1993**, *55−57*, 1221–1226. (c) Trznadel, M.; Pron, A.; Zagorska, M.; Chrzaszcz, R.; Pielichowski, J. *Macromolecules* **1998**, *31*, 5051–5058. (d) Demadrille, R.; Divisia-Blohorn, B.; Zagorska, M.; Quillard, S.; Rannou, P.; Traversa, J. P.; Pron, A. *New J. Chem.* **2003**, *27*, 1479–1484.

(17) Hall, D. G. In *Boronic Acids Preparation, Applications in Organic Synthesis and Medicine*; Hall, D. G., Ed.; Wiley-VCH: Weinheim, Germany, 2005; pp 1−99.

(18) Park, K. C.; Yoshino, K.; Tomiyasu, H. *Synthesis* **1999**, *12*, 2041–2044.

(19) Halvorsen, H.; Hope, H.; Skramstad, J. *Synth. Commun.* **2002**, *32*, 909–916.

127.94, 127.87, 127.76, 127.07, 124.37, 123.64, 123.31, 72.49, 48.08, 32.07, 22.10. FAB mass (*m*/*e*): calcd, 532.58; found, [M^+] 533.2.

meso-*(Benzo-[18-crown-6])bis(2,2′-bithienyl)methane. 4′-Formylbenzo-[18-crown-6]* (**4a**). 4′-Formylbenzo-[18-crown-6] (**4a**) was synthesized according to the following procedure. A mixture of 3,4-dihydroxybenzaldehyde (1 g, 7.24 mmol) and excess of K_2CO_3 (5.0031 g, 36.2 mmol) in DMF (∼50 mL) was stirred at ∼80 °C under N_2 for 30 min. Then, pentaethylene glycoldi-*p*-toluene sulfonate (3.483 mL, 7.9641 mmol) was added to the reaction mixture during 20 min and stirred at ∼80 °C under N_2 for 20 h. The cooled mixture was filtered. The filtrate was evaporated to dryness, and the residue was extracted with chloroform. The extract was evaporated to yield a viscous oil, which was purified by LC on a silica gel column with the $CHCl_3$/MeOH (98:2, v/v) eluent. Evaporation of the solvent yielded pale-yellow oil, which upon trituration with diethyl ether and refrigeration gave the desired product as a white solid. Yield: ∼75%. ^{1}H NMR ($CHCl_3$-*d*): δ(in ppm) 9.84 (s, 1H), 7.44 (dd, 1H, phenyl *H*), 7.39 (d, 1H, phenyl *H*), 6.95 (d, 1H, phenyl *H*), 4.28−4.18 (m, 4H, crownethylene *H*), 4.02−3.90 m, 4H, crownethylene *H*), 3.82−3.71 (m, 8H, crownethylene *H*), 3.69 (s, 4H, crownethylene *H*).

meso-*(Benzo-[18-crown-6])bis(2,2′-bithienyl) methane* (**4**). *meso*-(Benzo-[18-crown-6])bis(2,2′-bithienyl) methane (**4**) was prepared by mixing 2,2′-bithiophene (400 mg, 2.41 mmol) and **4a** (410.15 mg, 1.205 mmol) with ethylene glycol (40 mL), and the mixture was stirred for 20 min under N_2. Then, 60% $HClO_4$ (6 mL, 54.6 mmol) was added, and the mixture was stirred for 16 h at 60 °C. Next, the reaction mixture was cooled, filtered, and the obtained precipitate was washed with CH_2Cl_2. The resultant residue was washed with saturated Na_2CO_3, water, and then extracted with CH_2Cl_2. The organic phase was evaporated, and the collected oily residue was purified by LC on a silica gel column using hexane/$CHCl_3$ (20:80, v/v) as the eluent. Yield: 307 mg (39%). ^{1}H NMR ($CHCl_3$-*d*): δ(in ppm) 7.17 (dd, 2H, bithiophene *H*), 7.09 (dd, 2H, bithiophene *H*), 7.01 (d, 2H, bithiophene *H*), 6.99−6.96 (m, 2H, bithiophene *H*), 6.90−6.82 (m, 3H, benzocrown-phenyl *H*), 6.75 (dd, 2H, bithiophene *H*), 5.68 (s, 1H, −CH−), 4.19−4.10 (m, 4H, crownethylene *H*), 3.95−3.88 (m, 4H, crownethylene *H*), 3.80−3.67 (m, 12H, crownethylene *H*). ^{13}C NMR ($CHCl_3$-*d*): δ(in ppm): 149.13, 148.50, 146.68, 137.57, 136.94, 136.12, 127.88, 126.87, 124.34, 123.61, 123.24, 121.26, 114.70, 114.06, 71.02, 70.93, 69.82, 69.79, 69.35, 69.29. FAB mass (*m*/*e*): calcd, 654.89; found, [$M^+ + H_2O$] 671.9; calcd (with K^+), 693.99; found, [$M^+ + K^+$] 693.1.

Instrumentation, Techniques, and Procedures. *Cyclic Voltammetry (cv), Electrochemical Impedance Spectroscopy (eis), and Piezoelectric Microgravimetry (pm).* An AUTOLAB computerized electrochemistry system of Eco Chemie (Utrecht, The Netherlands) was used for the cyclic voltammetry (cv) and electrochemical impedance spectroscopy (eis) experiments. This system was equipped with the expansion cards of PGSTAT 12 potentiostat and frequency response analyzer (FRA). It was controlled by the GPES 4.9 software of Eco Chemie. A conventional three-neck V-shaped glass minicell of the working solution volume less than 0.5 mL was used in a three-electrode configuration. A 1 mm diameter soft glass shrouded Pt disk, Pt coil, and Ag|AgCl served as the working, auxiliary, and reference electrode, respectively.

Both the batch and flow piezoelectric microgravimetry (pm) experiments were performed by using the electrochemical quartz crystal microbalance, model EQCM 5710 and EQCM 5610, respectively, of the Institute of Physical Chemistry (Warsaw, Poland) under control of the EQCM 5710-S2 software of the same manufacturer. The AT-cut, plano-plano, 10 MHz quartz crystal resonator of 14 mm in diameter, coated on both sides with 5 mm diameter 100 nm thick sputtered Pt film electrodes, was used both as the working electrode and the sensor substrate. Prior to the polymer film electrodeposition, the resonators were cleaned with a piranha solution for 30 s (1:3, v/v; H_2O_2/H_2SO_4; caution: the piranha solution is dangerous in contact with skin or eye as it violently reacts with most organic compounds). The resonant frequency changes were measured with 1 Hz resolution. A Pt coil (EQCM 5710) or ring (EQCM 5610) as well as an AgCl film coated Ag wire (EQCM 5710) or ring (EQCM 5610) were used as the counter and pseudoreference electrode, respectively.

For electropolymerization, which was simultaneously performed under pm and cv batch conditions, EQCM 5710 was interfaced with the EP-20 potentiostat of the Institute of Physical Chemistry (Warsaw, Poland) and its quartz crystal holder was mounted horizontally with the quartz resonator facing upward in order to use as low volume of the sample solution as 100 μL.

UV−Visible Spectroscopy. The UV−visible spectra were recorded with 0.1 nm resolution by using a UV 2501-PC spectrophotometer of Shimadzu Corp. (Tokyo, Japan).

X-ray Photoelectron Spectroscopy (XPS). The XPS spectra were recorded with an Escalab-210 spectrometer of VG Scientific (East Grinstead, U.K.) by use of Al Kα ($h\nu$ = 1486.6 eV) X-ray radiation. The pressure in the spectrometer chamber was maintained at $\sim 5 \times 10^{-9}$ mbar. High-resolution scans were recorded with the 20 eV analyzer pass energy at a 0.1 eV increment for the N 1s core level spectra. The analyzer axis was normal to the surface. The spectra were analyzed by the Avantage data system software of Thermo Electron Corp. (East Grinstead, U.K.).

Flow Injection Analysis (FIA). The Pt/quartz resonator, coated either with the MIP or nonimprinted polymer (NIP) film (see below in Sensor Fabrication), was mounted in the flow-through EQCM 5610 holder to examine analytical performance of the sensor under FIA conditions.[20] A HEPES buffer (pH = 7.5), used as the career solution, was pumped through the holder with the syringe pump model KDS100 of KD Scientific, Inc. (Holliston, MA). The FIA experiments were carried out either at a low (35) or high (150 μL/min) flow rate. Samples of the analyte, dissolved in the buffer solution of the same composition as that of the carrier solution and the volume of 100 μL or 1 mL, were injected with use of the rotary six-port valve model 7725i of Rheodyne, (Cotati, CA).

Sensor Fabrication. The recognition film of the chemosensor was composed of two layers. These were deposited, by electropolymerization under cv conditions, one on top of the other.

The first layer was a poly(bithiophene) barrier film. It was deposited by potential cycling at 50 mV/s, in the potential range

(20) Kochman, A.; Krupka, A.; Grissbach, J.; Kutner, W.; Gniewinska, B.; Nafalski, L. *Electroanalysis* **2006**, *18*, 2168–2173.

0.5−1.5 V, from 1 mM bithiophene and 0.05 M (TBA)ClO_4, in acetonitrile or 1,2-dichlorobenzene. The growth of this polymer was controlled by the number of cv cycles. After the potential cycling was seized, the polymer was rinsed with acetonitrile in order to remove excess of the supporting electrolyte.

The thickness of the barrier film was estimated based on the frequency change vs potential curves recorded during electrodeposition. Full electrode coverage with the bithiophene monolayer is close to 3.8×10^{-11} mol/m^2, i.e., 6.38 ng, assuming ~0.89 nm diameter of the bithiophene molecule. The mass of the poly(bithiophene) barrier film deposited was determined from the resonant frequency change during electrodeposition of this film by using the Sauerbrey equation. The total number of layers deposited was determined by dividing this value by the mass of a monolayer of bithiophene. Thickness of the poly(bithiophene) film was estimated from the thickness of the monolayer, taken as 0.89 nm, and multiplied by the number of monolayers.

The MIP film served as the second, outermost, layer. This film was prepared by electropolymerization of **3**, **4**, and histamine at the mole ratio of 2:2:1 in 0.1 M (TBA)ClO_4 and TFA in acetonitrile. After electropolymerization, the MIP film was rinsed with acetonitrile to remove the supporting electrolyte. The histamine template was then extracted by washing the MIP film with 0.01 M NaOH for 12 h. Completeness of this extraction was confirmed by the UV−vis spectroscopic and XPS measurements. NIP, used as a control polymer, was prepared in the absence of histamine by using the same procedure.

RESULTS AND DISCUSSION

First, a poly(bithiophene) barrier film was electropolymerized on the Pt/quartz electrode. Next, the histamine-templated MIP film was deposited on top of this barrier film by electrochemical copolymerization of the self-assembled complex of histamine with functional monomers **3** and **4**. Then, the template was extracted from the MIP film with NaOH. The presence or absence of the histamine template in the MIP film was confirmed by UV−vis and X-ray photoelectron spectroscopy. Subsequently, the histamine analyte was determined, and the analytical performance of the chemosensor was characterized at the template-free MIP film under FIA conditions with the pm detection.

Electrochemical Polymerization and Characterization of MIP and NIP Films. On the cyclic voltammogram of the first cycle for histamine, recorded at the Pt disk electrode (Curve 1 in Figure 1), the anodic peak at ~0.80 V corresponds to the irreversible electro-oxidation of histamine.[21,22] This peak diminished in subsequent cycles (not shown) as products of this reaction were adsorbed on the electrode surface contaminating it and blocking.[22]

Figure 2a shows the cv curve of the first cycle for histamine imprinting by electrochemical copolymerization of **3** and **4** in 0.1 M (TBA)ClO_4, 8.64 nM TFA, in acetonitrile (pH = 8.0), in the presence of the histamine template, on the Pt/quartz electrode. The anodic peak at ~0.80 V and the broad and poorly

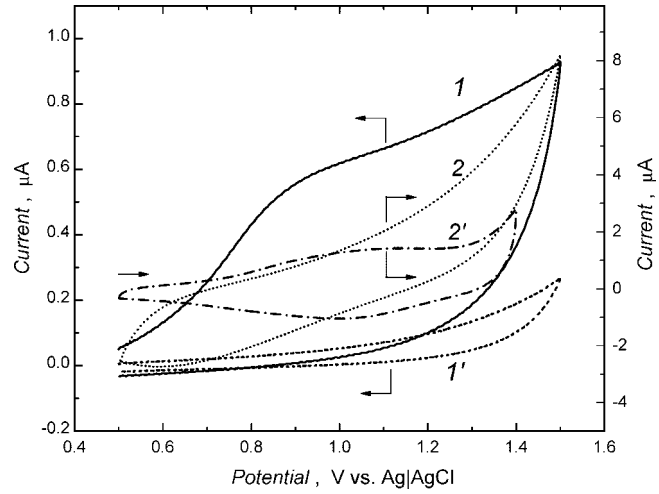

Figure 1. Cyclic voltammograms for 1 mM histamine in 0.1 M (TBA)ClO_4, in acetonitrile, at (1) the Pt disk electrode and (2) the 200 nm thick poly(bithiophene) barrier film coated Pt disk electrode. Curves (1′) and (2′) represent cyclic voltammograms of the blank supporting electrolyte solutions at the Pt disk electrode and the 200 nm poly(bithiophene) coated Pt disk electrode, respectively. Potential scan rate was 50 mV/s.

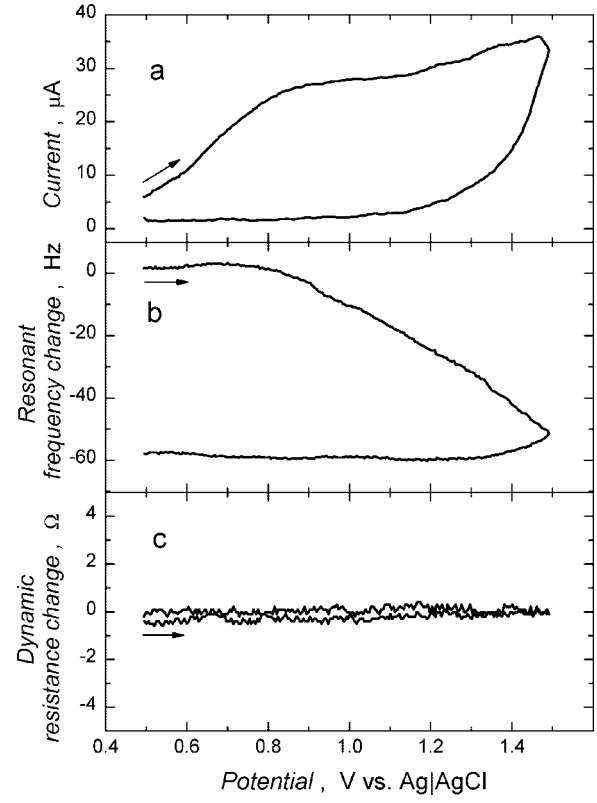

Figure 2. Simultaneously recorded curves of (a) cyclic voltammetry, (b) resonant frequency change vs potential, and (c) dynamic resistance change vs potential for electropolymerization of 1 mM **3**, 1 mM **4**, and 0.5 mM histamine on the Pt/quartz electrode in 0.1 M (TBA)ClO_4 and 8.64 nM trifluoroacetic acid, in acetonitrile (pH = 8.0). The potential scan rate was 50 mV/s.

developed current−potential shoulder at around 1.30 V, both decreasing in subsequent cycles (not shown), correspond to histamine electro-oxidation and electropolymerization of the monomers, respectively. The growth of the MIP film is manifested by the simultaneously recorded corresponding

(21) Manica, D. P.; Mitsumori, Y.; Ewing, A. G. *Anal. Chem.* **2003**, *75*, 4572–4577.
(22) Sarada, B. V.; Rao, T. N.; Tryk, D. A.; Fujishima, A. *Anal. Chem.* **2000**, *72*, 1632–1638.

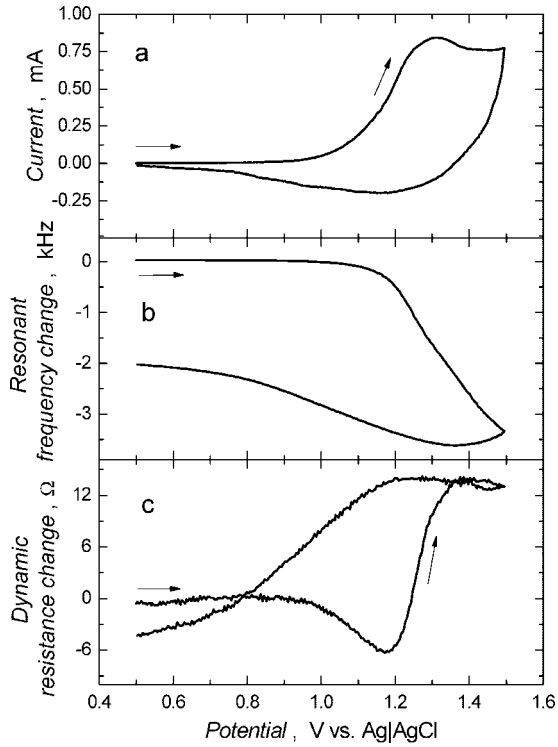

Figure 3. Simultaneously recorded curves of (a) cyclic voltammetry, (b) resonant frequency change vs potential, and (c) dynamic resistance change vs potential for electropolymerization of 1 mM **3**, 1 mM **4**, and 0.5 mM histamine in 0.1 M $(TBA)ClO_4$ and 8.64 nM trifluoroacetic acid, in acetonitrile (pH = 8.0), on the 200 nm thick poly(bithiophene) barrier film coated Pt/quartz electrode. The potential scan rate was 50 mV/s.

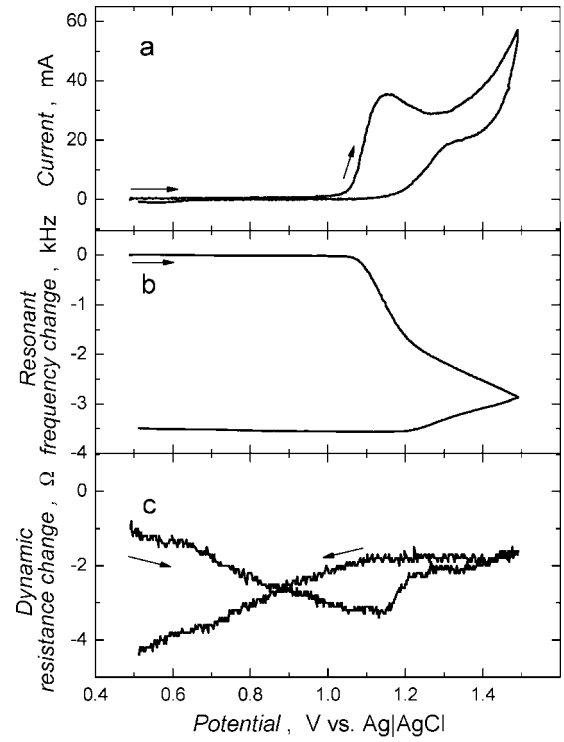

Figure 4. Simultaneously recorded curves of (a) cyclic voltammetry, (b) resonant frequency change vs potential, and (c) dynamic resistance change vs potential for electropolymerization of 1 mM **3** and 1 mM **4** in 0.1 M $(TBA)ClO_4$ and 8.64 nM trifluoroacetic acid, in acetonitrile (pH = 8.0), on the Pt/quartz electrode. The potential scan rate was 50 mV/s.

frequency decrease (Figure 2b). Apparently, histamine is electro-oxidized at the potential lower than that necessary for the electropolymerization and, therefore, it may be not available in its genuine form, in the electrode vicinity, for imprinting. So, the obtained imprinted sites may not necessarily be complementary to those of the histamine template but, equally well, to its electro-oxidation products. No noticeable shift in the simultaneously recorded dynamic resistance change with the potential swept (Figure 2c) indicates no change in the MIP film rigidity.

For improvement in imprinting, clearly, electro-oxidation of the histamine template should be eliminated in order to prevent its consumption in the electrode process and the electrode fouling by its oxidation products. Most rationally, the electrode surface should be inaccessible to histamine. For that purpose, a conducting poly(bithiophene) film of optimum thickness was employed to serve as a barrier for the histamine diffusion to the electrode surface and electro-oxidation. Curve 2 in Figure 1 shows a cv response to histamine of the poly(bithiophene) film coated Pt disk electrode. Here, the anodic peak corresponding to electro-oxidation of histamine is almost vanished indicating the effective redox blocking property of this film. Therefore, the histamine-templated MIP film was deposited in subsequent studies on top of this barrier film by electrochemical copolymerization of the histamine complex with the functional monomers **3** and **4** (Scheme 2). Noticeably, the anodic peak at ~1.30 V (Figure 3a) indicates electropolymerization and efficient imprinting of histamine, as evidenced by the frequency decrease (Figure 3b) corresponding to the MIP film deposition. The initial decrease at ~1.0 V, followed by the increase in the dynamic resistance change with the anodic potential increase (Figure 3c) at around 1.20 V, are most plausibly due to the egress of cations and ingress of anions of the supporting electrolyte, substantiating the rigidity variations of the MIP film.

Figure 4 illustrates preparation of a control NIP film by electrochemical polymerization of **3** and **4** in the absence of histamine. Here, the anodic peak at ~1.15 V, which increases in subsequent cycles (not shown), indicates that the electropolymerization (Figure 4a) proceeds vigorously. Simultaneously, the resonant frequency change distinctly decreases (Figure 4b). The electrodeposition results in changes in the visco-elasticity of the NIP film, as indicated by the variation in the dynamic resistance change (Figure 4c) due to insertion and removal of ions of the supporting electrolyte. Further, the control NIP film was electropolymerized, for comparison, on top of the poly(bithiophene) barrier film coated Pt electrode in the absence of the histamine template (not shown).

Effect of Thickness of the Poly(bithiophene) Barrier Film on the MIP Film Performance. The underlying barrier film should effectively block electro-oxidation of histamine. For that purpose it should be sufficiently thick. Therefore, we performed systematic studies on simultaneous cv, pm, and dynamic resistant change vs potential of histamine imprinting in the polymer film electrodeposited onto the poly(bithiopene) barrier film of different thickness. For instance, for a 90 nm thick poly(bithiopene) film, the voltammogram of the first cycle shows two broad anodic peaks

at around 0.80 and 1.0 V and one well developed peak at ~1.30 V (Figure S1′a in the Supporting Information). The first peak is characteristic of histamine electro-oxidation indicating that the barrier film is insufficiently thick to block the histamine electro-oxidation. Apparently, two different electrochemical processes proceed simultaneously, i.e., histamine electro-oxidation and electrochemical copolymerization of the **3** and **4** monomer. These processes are clearly visualized in the frequency change vs potential curve (Figure S1′b in the Supporting Information). The first frequency decrease at ~0.80 V is due to the histamine electro-oxidation and the counterion ingress to the film while the other at ~1.30 V to the electropolymerization. However, this latter decrease, although as large as 500 Hz, is insufficient to ensure efficient imprinting of histamine. This is because the cv current decreases in subsequent cycles (not shown) meaning that electro-oxidation of the histamine template prior to the MIP formation results in contamination of the electrode surface with its oxidation products. Moreover, unavailability of histamine in its pristine form leads to inadequate imprinting in subsequent MIP electropolymerization. The imprinting can thus be improved by using thicker underlying poly(bithiophene) film in order to block the histamine electro-oxidation. Figure 3 shows the MIP preparation on top of an ~200 nm thick poly(bithiopene) film. The lack of the anodic peak at ~0.80 V in this case proves that histamine electro-oxidation has been eliminated. A distinct anodic peak at ~1.30 V corresponding to electropolymerization of the monomers evidences very effective imprinting. The simultaneous pronounced frequency decrease of ~3.5 kHz (Figure 3b) ensures deposition of the desired MIP film. Ongoing discussion will be based on the sensing capabilities of the Pt/quartz electrodes coated with the MIP films in the presence and absence of the 200 nm thick poly(bithiophene) barrier film.

Extraction of the Histamine Template from the MIP Film. After electropolymerization, the MIP film was, first, rinsed thoroughly with acetonitrile to remove all physisorbed species. The volume of the MIP film was estimated as ~1.58 nL based on the frequency change vs potential curves recorded during electrodeposition of the film and assuming 1.1 g/cm^3 density of poly(bithiophene).[23] The histamine template was removed from MIP by extraction with NaOH. The resulting mass loss of the film served to determine concentration of the molecular cavities in MIP accessible for the histamine analyte. Advantageously, this concentration was high and equal to ~1.10 M. Completeness of the template removal was confirmed by the XPS and UV−vis spectroscopy measurements before and after the extraction.

In the XPS measurements, the binding energy of nitrogen N 1s has been used as a benchmark for the histamine presence in the imprinted molecular cavities of the MIP film. A binding energy profile for the MIP film before and after histamine extraction is shown in Figure 5a and 5b, respectively. The composed band at around 400.3 eV corresponds to nitrogen atoms of histamine in different environments. The deconvoluted spectrum shows bands at 402.5, 403.1, and 404.6 eV, corresponding to the protonated nitrogen atom of the aliphatic amine moiety (−NH_3^+), hydrogenated (−NH−) and nonhydrogenated (−N=) nitrogen atom

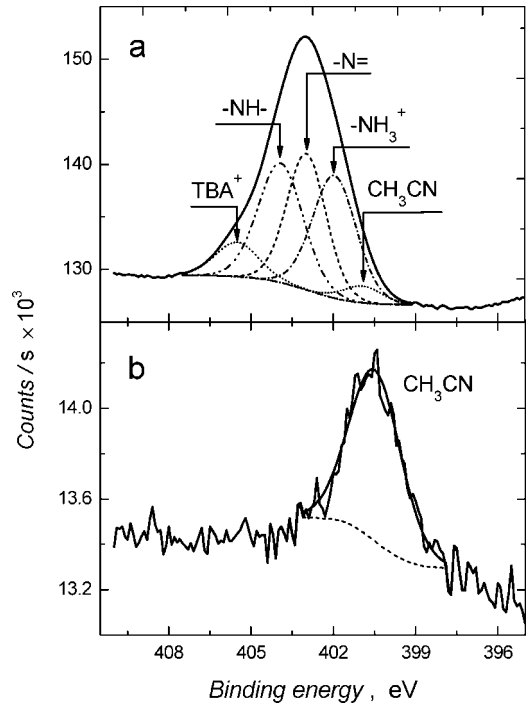

Figure 5. X-ray photoelectron spectroscopy (XPS) spectra of N 1s for the histamine-templated MIP film, deposited by electropolymerization on the Pt/quartz electrode, (a) before and (b) after histamine extraction with 0.01 M NaOH. Assignments of the nitrogen atoms of histamine for deconvoluted peaks are indicated at curves. The conditions of preparation of the histamine-templated MIP film as in Figure 4.

of the imidazole moiety, respectively, of histamine (Figure 5a).[24] The band corresponding to the nonhydrogenated (−N=) nitrogen atom is shifted to higher binding energies with respect to that reported.[24] Presumably, this shift is due to interaction of −N= with the boron atom of the dioxaborinane moiety of MIP. The band at 405.5 eV stands for the nitrogen atom of trace quaternary ammonium cation, (TBA^+),[25] of the supporting electrolyte entrapped within the MIP film during electrodeposition. The XPS spectrum for the MIP film, after extensive washing with NaOH, reveals a very weak band at 400.6 eV attributed to the nitrogen atom of the acetonitrile[26] solvent (Figure 5b). Overall, the absence of bands corresponding to the histamine nitrogen atoms in the spectrum for the film after extraction assures completeness of the histamine removal.

In the UV−vis spectral measurements (Figure 6), the histamine template was removed from MIP by soaking it in 0.01 M NaOH for 12 h and histamine was detected in the extract. In the UV−vis spectrum for the NaOH extracting solution (curve 2 in Figure 6) the band at around 217 nm corresponds to histamine (Curve 1 in Figure 6). A complete removal of histamine from the film has been confirmed by the absence of this band (curve 3 in Figure 6) after a five-time consecutive rinsing of the film with 0.01 M NaOH. In order to remove possible adsorbed impurities or solvent, the template-free MIP film was eventually washed with water before its further use.

(23) Skompska, M.; Jackson, A.; Hillman, A. R. *Phys. Chem. Chem. Phys.* **2000**, *2*, 4748–4757.

(24) Bradley, R. H.; Ling, X.; Sutherland, I.; Beamson, G. *Carbon* **1994**, *32*, 185–186.

(25) Wojtowicz, M. A.; Pels, J. R.; Moulijn, J. A. *Fuel* **1995**, *74*, 507–516.

(26) Zheng, W. T.; Xing, K. Z.; Hellgren, N.; Lögdlund, M.; Johansson, Å.; Gelivs, U.; Salaneck, W. R.; Sundgren, J.-E. *J. Electron Spectrosc. Relat. Phenom.* **1997**, *87*, 45–49.

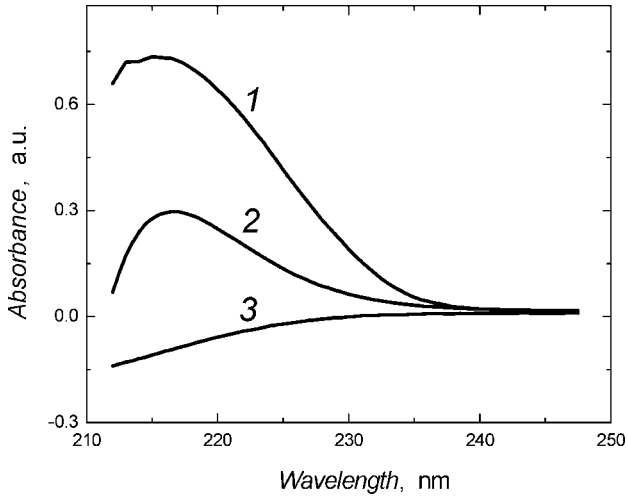

Figure 6. The UV−vis spectra for the 0.01 M NaOH solution of (1) 1 μM histamine, (2) the first extraction of the histamine-templated MIP film, and (3) the fifth extraction of the histamine-templated MIP film. The conditions of preparation of the MIP film as in Figure 4.

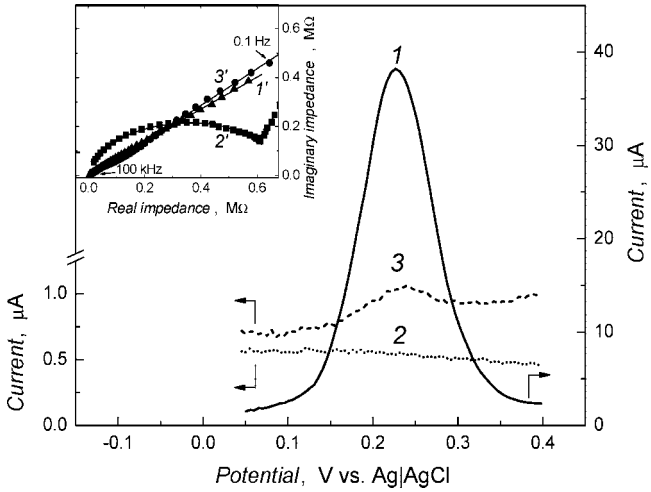

Figure 7. Differential pulse voltammograms for 1 mM $K_4Fe(CN)_6$ in 0.1 M NaCl at (1) the bare Pt/quartz electrode as well as the Pt/quartz electrode coated with the poly(bithiophene) barrier film overlaid with the histamine-templated MIP film (2) before and (3) after histamine extraction with 0.01 M NaOH. The step potential was 5 mV; pulse amplitude was 25 mV; pulse width was 50 ms. Inset presents complex-plane impedance plots of the electrochemical impedance spectroscopy (eis) for 1 mM $K_4Fe(CN)_6$ in 0.1 M NaCl at (1′) the bare Pt disk electrode as well as at the Pt disk electrode coated with the histamine-templated MIP film (2′) before and (3′) after histamine extraction with 0.01 M NaOH. The eis frequency ranged from 0.1 Hz to 1.0 kHz. The conditions of preparation of the MIP film as in Figure 4.

Electrochemical Characterization of the MIP Film Coated Resonator Transducers. The MIP film has electrochemically been characterized with the use of the $Fe(CN)_6^{3-}/Fe(CN)_6^{4-}$ redox probe in order to unravel its morphological features. The dpv curves for 1 mM $K_4Fe(CN)_6$ in 0.1 M NaCl at the Pt/quartz resonator uncoated and coated with the MIP film is shown in Figure 7. For the latter, the 200 nm thick poly(bithiophene) barrier film was deposited by electropolymerization on the Pt/quartz electrode before the MIP film electrodeposition. At the bare Pt/quartz electrode, a well developed dpv peak for the $Fe(CN)_6^{3-}/Fe(CN)_6^{4-}$ couple (Curve 1 in Figure 7) indicates facile electron transfer. However, these peaks are largely decreased at the Pt/quartz electrode coated with the MIP film containing the histamine template (Curve 2 in Figure 7). Apparently, this template-loaded MIP film is effectively blocking the electrode surface. Curve 3 in Figure 7 is the voltammogram for the Pt/quartz electrode coated with the same MIP film after extensive histamine extraction with 0.01 M NaOH. Under these conditions, the dpv peak is relatively increased, as compared to that in curve 2, like if some channels were opened that way for analyte diffusion through the MIP film. Most likely, the template extraction empties the histamine imprinted molecular cavities thus enhancing permeability of the MIP with respect to the redox probe.

Resistive properties of the MIP films have been characterized by eis. The inset in Figure 7 shows the plot of complex-plane impedance for the MIP film coated Pt/quartz electrode in 1 mM $K_4Fe(CN)_6$, in 0.1 M NaCl. Curve 1′ in this inset is the dependence of the imaginary vs real part of impedance for the bare Pt/quartz electrode. A straight line of the $\pi/4$ slope obtained indicates that the electron transfer kinetics is unhindered and solely controlled by the rate of diffusion of the $Fe(CN)_6^{4-}$ redox probe. In contrast, the plot for the histamine-containing MIP film coated electrode (Curve 2′ in the inset to Figure 7) comprises an arc and a straight line in the high and low frequency range, respectively. Solid plots are curves simulated by using the Randles equivalent circuit. The diameter of this arc is higher the higher is the charge transfer resistance.[27] Accordingly, the apparent charge transfer resistance of the Pt/quartz electrode coated with histamine-containing MIP film (0.75 MΩ) is much higher than that of the uncoated electrode (0.2 kΩ). If the slope of the straight line is higher, then lesser is the porosity of the electrode.[28] At this modified electrode, the $Fe(CN)_6^{3-}/Fe(CN)_6^{4-}$ electrode process is hindered in the high frequency range, presumably due to the presence of the histamine-loaded MIP film obstructing diffusion of the probe. Curve 3′ in the inset to Figure 7 shows the plot of the complex-plane impedance for the template-extracted, MIP film coated, Pt/quartz electrode. Curve 3′ resembles Curve 2′, except that diameter of the arc in the high frequency domain is much smaller than that in Curve 2′ indicating lower charge transfer resistance (0.21 MΩ) of the film-coated electrode. Moreover, the slope of the straight line is smaller than that in curve 3′ as if the MIP film became more porous after the template removal. Evidently, removal of the template leaves imprinted molecular cavities open facilitating the diffusion of the redox probe through the MIP film to the electrode. Consequently, the electron transfer is less hindered.

Analytical Performance of the MIP/QCM Chemosensor for Histamine. *Histamine Determination.* Interactions of the histamine analyte with the binding sites of the MIP film coating the Pt/quartz resonator has been studied under FIA conditions. These interactions are assumed to be mainly due to the complementarity in stereo geometry between histamine and the imprinted molecular cavities of MIP on the one hand and to electrostatic

(27) Lasia, A. In *Modern Aspects of Electrochemistry*; Conway, B. E., Bockris, J., White, R. E., Eds.; Kluwer Academic/Plenum: New York 1999; Vol. 32, pp 143−248.
(28) DeLevie, R. In *Advances in Electrochemistry and Electrochemical Engineering*; Delahay, P., Tobias, C. W., Eds.; John Wiley: New York, 1967; Vol. u6, pp 329−397.

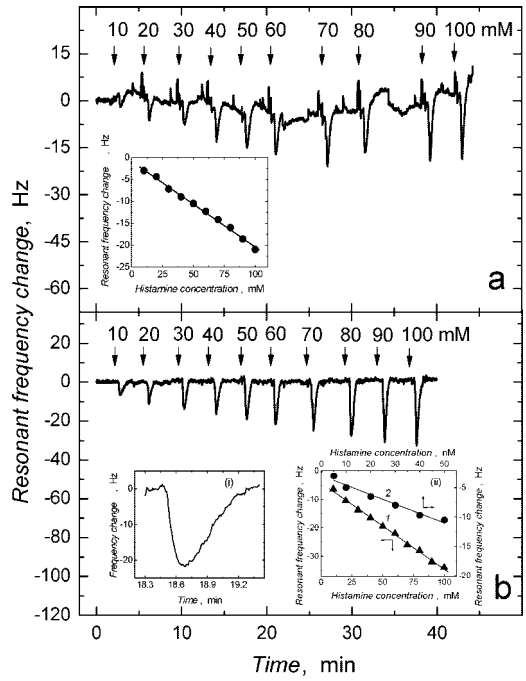

Figure 8. Resonant frequency changes with time due to repetitive FIA injections of histamine in 0.5 M HEPES buffer (pH = 7.5), for the MIP film electrodeposited on (a) the bare Pt/quartz electrode and (b) the 200 nm thick poly(bithiophene) barrier film coated Pt/quartz electrode. Volume of the injected histamine solution was 100 μL. Histamine concentration is indicated with a number at each peak. The flow rate of the carrier solution of 0.5 M HEPES buffer (pH = 7.5) was 150 μL/min. The conditions of preparation of the MIP film were the same as in Figure 4. The inset in (a) is the histamine calibration plot for the sample volume of 100 μL and the flow rate of 150 μL/min. Inset (i) in (b) is the resonant frequency change with time for the MIP film electrodeposited on the 200 nm thick poly(bithiophene) barrier film coated Pt/quartz electrode after injection of a 100 μL sample of the 60 mM histamine in 0.5 M HEPES buffer (pH = 7.5). Inset (ii) in (b) is the histamine calibration plot for the injected sample volume and flow rate of (1) 100 μL and 150 μL/min as well as (2) 1 mL and 35 μL/min, respectively.

interactions between the histamine and MIP binding sites on the other. For effective interaction with MIP, the histamine binding sites should be available. That is, the nitrogen atom of the imidazole moiety should remain nonhydrogenated, and the primary amine group of the aliphatic amine moiety should be protonated. Hence, acidity of the working solution greatly influences performance of the chemosensor playing a decisive role both in the histamine imprinting and determination step. Therefore, it should be kept in the range $pK_{a1} < pH < pK_{a2}$ (Scheme 1). Accordingly, the histamine was determined at pH = 7.5 using an aqueous 0.5 M HEPES buffer as the carrier solution. When the solution flows over the MIP film, the interactions between the histamine analyte and the MIP binding sites result in the mass of the film increase causing the resonant frequency decrease.

The frequency change vs time responses to repetitive FIA injections of the histamine sample solution for the MIP film deposited in the absence and presence of the 200 nm thick poly(bithiophene) barrier film is shown in Figure 8a and 8b, respectively. Upon injection of histamine, first, the frequency decreases abruptly [inset (i) to Figure 8b] due to the histamine interaction with the MIP binding sites. The response time, i.e., time at which the signal reaches 90% of its maximum value, was as short as $\tau_{90\%} = 18$ s [inset (i) to Figure 8b]. Then, the signal relatively quickly returned to its initial value as histamine was washed away from MIP with the excess of the carrier solution. So, the recovery time was also very short and equal to ~60 s. Moreover, histamine binding is, advantageously, perfectly reversible. Generally, the strength of interactions and the magnitude of the mass transfer resistance of MIP affect both the time of interaction and recovery. The higher the histamine concentration the higher is the peak of the negative frequency change. Importantly, the peaks are better developed and sensitivity is higher in the presence rather than absence of the 200 nm thick poly(bithiophene) barrier film [inset (ii) to Figure 8b]. The initial parts of the frequency−time profiles corresponding to the analyte ingress were used to determine stability constants of the MIP−analyte complexes (see below in the Selectivity section).

Table 1. Flow Injection Analysis Sensitivity with Respect to Histamine of the NIP and Histamine-Templated MIP Chemosensors Featuring the 90 or 200 nm Thick or No Poly(bithiophene) Barrier Film[a]

sensor architecture	sensitivity (±0.01 std deviation) Hz/mM	correlation coefficient
MIP/200 nm poly(bithiophene)/Pt/quartz	−0.33	0.998
MIP/Pt/quartz	−0.15	0.997
NIP/200 nm poly(bithiophene)/Pt/quartz	−0.08	0.997
MIP/90 nm poly(bithiophene)/Pt/quartz	−0.41	0.996
NIP/90 nm poly(bithiophene)/Pt/quartz	−0.34	0.997

[a] 150 μL/min flow rate; 100 μL sample volume.

Sensitivity and Detectability. The calibration plots for histamine determination (inset (ii) in Figure 8b) have been constructed based on FIA peaks. For the 150 μL/min flow rate and 100 μL volume of the injected sample solution the sensitivity values calculated from slopes of the calibration plots are summarized in Table 1. Importantly, sensitivity of the chemosensor featuring the 200 nm thick poly(bithiophene) barrier film [line 1 in inset (ii) to Figure 8b] is over twice as high as that of the sensor deprived of this film (inset to Figure 8a). The linear concentration range extends from 10 to 100 mM. Notably, sensitivity of the chemosensor featuring the control NIP film electropolymerized on top of the 200 nm thick poly(bithiophene) barrier film was more than 4 times lower (Table 1). Apparently, the presence in the polymer of the binding sites imprinted for histamine is decisive for the analyte determination substantiating capability of the imprinting for the sensing performance.

Detectability of the chemosensor was determined under suitably selected conditions in another set of FIA experiments. That is, the flow rate was maintained as low as 35 μL/min, and the volume of the sample was as large as 1 mL [line 2 in inset (ii) to Figure 8b]. The resulting detection limit in terms of the histamine concentration was 5 nM at the signal-to-noise ratio of 3.

Thickness of the barrier film plays a crucial role both in histamine imprinting and determination. For instance, for a poly(bithiophene) film as thin as 90 nm, sensitivity of the MIP

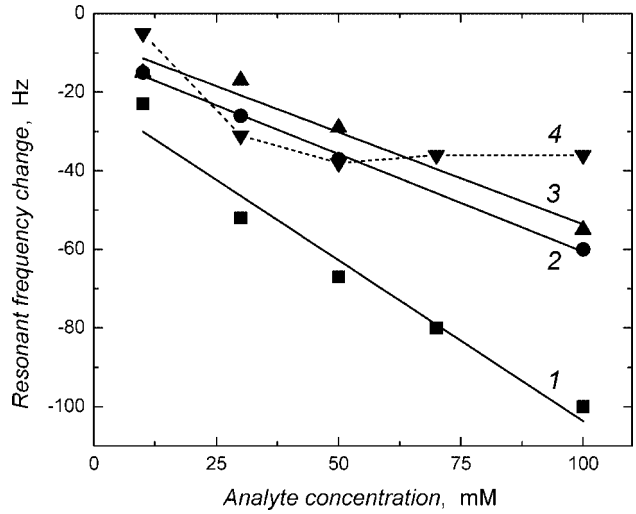

Figure 9. FIA calibration plots for (1) histamine, (2) tryptamine, (3) dopamine, and (4) imidazole for the histamine-templated MIP film, electropolymerized on the 200 nm thick poly(bithiophene) barrier film. The volume of the injected sample solution was 100 μL. The flow rate of the carrier 0.5 M HEPES buffer (pH = 7.5) solution was 35 μL/min. The histamine template was extracted from the MIP film with 0.01 M NaOH before determinations.

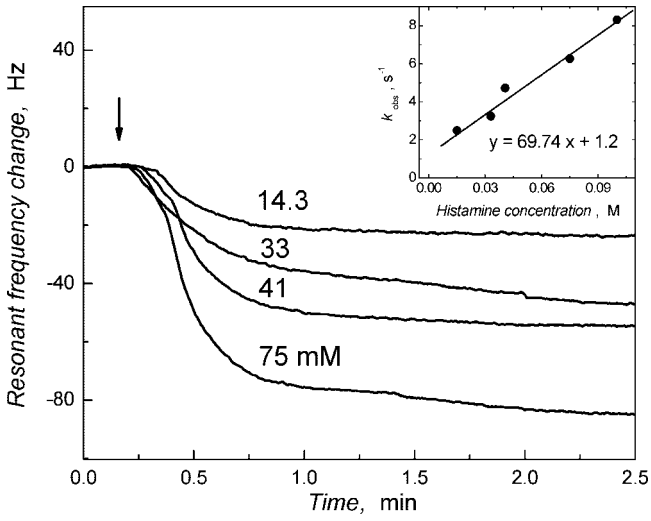

Figure 10. Initial resonant frequency changes with time due to FIA histamine injection, for the histamine-templated MIP film, electrodeposited on the 200 nm thick poly(bithiophene) barrier film-coated Pt/quartz electrode. Flow rate of the carrier 0.5 M HEPES buffer (pH = 7.5) solution was 150 μL/min. Volume of the injected sample of histamine in 0.5 M HEPES buffer (pH = 7.5) was 1 mL. The inset is the dependence of k_{obs}, calculated by nonlinear fitting of the association parts of the binding curves, on the corresponding concentration of the histamine analyte. The histamine template was extracted from the MIP film with 0.01 M NaOH before injecting the histamine analyte. The vertical arrow indicates the injection time.

and NIP based chemosensor is similar (Figure S2 in the Supporting Information) indicating incomplete or poorly defined imprinting. Apparently, so thin poly(bithiophene) barrier film fails to prevent histamine from electro-oxidation prior to imprinting. Instead, products of this electro-oxidation are most likely imprinted and, presumably, binding sites are formed that are unable to effectively interact with histamine.

Table 2. Flow Injection Analysis Sensitivity with Respect to the Histamine Analyte and Different Interfering Agents of the Histamine-Templated MIP Chemosensor Featuring the 200 nm Thick Poly(bithiophene) Barrier Film on the Pt/Quartz Resonator[a]

determined compound	sensitivity (±0.05 std deviation) Hz/mM	correlation coefficient
histamine	−0.86	0.987
tryptamine	−0.48	0.988
dopamine	−0.46	0.988
imidazole	−0.49	0.986

[a] 35 μL/min flow rate; 1 mL sample volume.

Selectivity. For evaluation of selectivity of the histamine-templated MIP film, cross reactivity with respect to functionally and structurally similar interfering agents, such as tryptamine, dopamine, and imidazole, was compared. The respective FIA calibration plots of the frequency change vs concentration of the injected compound are shown in Figure 9. The highest sensitivity was obtained for histamine (Table 2). It was twice as high as that for dopamine and tryptamine, manifesting selectivity of the sensor with respect to common interfering agents. Apparently, stability of the respective MIP and analyte (A) complex (MIP−A) decreases in the same order (see below). Interactions of imidazole with histamine-templated MIP saturate at concentration of ~50 mM, plausibly due to incompatibility of the MIP binding sites to those of the imidazole molecule.

The MIP film forms an affinity complex with an analyte. In effect, the mass of the film increases and, hence, the measured resonant frequency decreases. Toward selectivity studies, values of the stability constant, K_s, of complexes of MIP and the analyte or interfering agent were determined. The rate of formation and decomposition of the MIP−A complex is described by the rate constant of association, k_a, and dissociation, k_d, respectively.[29] The resulting equilibrium can be expressed as

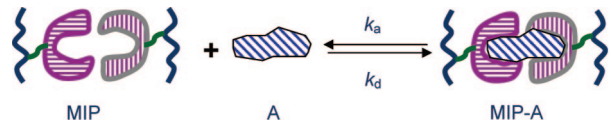

(1)

The rate of formation of the MIP−A complex can be represented by the measured frequency change and concentration of the injected analyte, c_A,

$$d[\text{MIP}-\text{A}]/dt = -B(df/dt) = K_a C_A(f_{max} - f) - K_d f \quad (2)$$

where $B = -[(A(\mu_q\rho_q)^{1/2}/2)f_0^2 M_w V]$ is the proportionality factor derived from the Sauerbrey equation, f_0 is the resonant frequency of the unperturbed quartz resonator, μ_q is the shear modulus of the AT-cut quartz crystal, ρ_q is the density of quartz, A is acoustically active area of the resonator, M_w is the molecular weight of the MIP−A complex, V is the volume of the MIP film, f_{eq} is the equilibrium frequency at time t, and f_{max} is the maximum shift in the resonant frequency for the analyte injection at a particular concentration. By integrating eq 2 with respect to time, then substituting

$$f_{eq} = k_a c_A f_{max}/(k_a c_A + k_d) \quad (3)$$

and

$$k_{obs} = k_a c_A + k_d \quad (4)$$

one obtains eq 5[30]

$$f_{eq} = f_{max}[1 - \exp(-k_{obs}t)] \quad (5)$$

$$K_s = K_a/K_d \quad (6)$$

Shifts of the experimental frequency change with time were fitted to kinetic eq 5. From the fitting parameters, k_{obs} was calculated. The initial change of the resonant frequency, recorded immediately after FIA injection of the analyte, was used for this analysis. In order to eliminate the contribution originating from the signal dispersion caused by the FIA system, chronoamperometric control experiments were performed, under FIA conditions, with the use of the bare Pt/quartz electrode and the $Fe(CN)_6^{3-}/Fe(CN)_6^{4-}$ electroactive probe. The normalized chronoamperometric curves for this probe were subtracted from the normalized resonant frequency change vs time curves recorded for the interaction of the injected analyte with the MIP film coated Pt/quartz resonator. Figure 10 shows the corrected curves of the initial resonant frequency change with time for the FIA injections of histamine samples of different concentrations. From the ratio of the slope and intercept of the linear plot of k_{obs} vs histamine concentration constructed and eq 6 (inset to Figure 10), the K_s value for the MIP−histamine complex was calculated as 57.0 M^{-1}. The determined K_s value is 9 and 5 times higher than that of the stability constant determined for the MIP−dopamine (6.4 M^{-1}) and MIP−tryptamine complex (10.7 M^{-1}), respectively. Clearly, interactions of the histamine analyte with the MIP binding sites complementary to those of the histamine molecule are stronger than those of the functionally or structurally related interfering agents.

CONCLUSIONS

The MIP film, used as the analyte recognition element, combined with the thickness-shear-mode bulk-acoustic-wave resonator, used as the piezoelectric signal transducer, has proven its utility as a chemosensor for determination of histamine. The presence of the poly(bithiophene) barrier film largely improves performance of the chemosensor. For superior sensitivity and selectivity, this film should be at least 200 nm thick in order to effectively prevent electro-oxidation of histamine. Under carefully selected FIA conditions, the concentration lower limit of detection was as low as 5 nM histamine. This value corresponds to the lower limit of histamine concentration in the human body, i.e., 4.48−13.45 nM, under normal conditions. In the case of anaphylactic shock (anaphylaxis), the histamine concentration is much higher. The sensor is selective with respect to functionally and structurally related interfering compounds, such as tryptamine, dopamine, and imidazole. The stability constants of the MIP complexes of histamine, dopamine, and tryptamine reveal that the imprinted site bindings of histamine is much stronger than its interfering agents.

(29) Skladal, P. *J. Braz. Chem. Soc.* **2003**, *14*, 491–502.
(30) (a) Halamek, J.; Hepel, M.; Skladal, P. *Biosen. Bioelectron.* **2001**, *16*, 253. (b) Pribyl, J.; Hepel, M.; Skladal, P. *Sens. Actuators, B* **2006**, *113*, 900.

ACKNOWLEDGMENT

We acknowledge Dr. A. Kosinski for help with the XPS measurements and Prof. A. Sadkowski for discussion. The authors are thankful to the Ministry of Science and Higher Education of Poland (Project 548/6.PR UE/2008/7 to W.K.) and National Science Foundation (Grant CHE 0804015 to F.D.S.) for support of this work. S.S. is also grateful to the European Commission for financial support through the *Nanomaterials for Application in Sensors, Catalysis and Emerging Technologies*, NASCENT, Project within the Marie Curie Research Training Network (Contract No. MRTN-CT-2006-033873).

NOTE ADDED AFTER ASAP PUBLICATION

This article was released ASAP on March 11, 2009 with minor typographical errors. The correct version was posted on March 31, 2009.

SUPPORTING INFORMATION AVAILABLE

Additional information as noted in the text. This material is available free of charge via the Internet at http://pubs.acs.org.

Received for review December 4, 2008. Accepted February 15, 2009.

AC8025652